A Preventative Approach to Mitigating CW Interference in GPS Receivers

A Preventative Approach to Mitigating CW Interference in GPS Receivers

ASGHAR TABATABAEI BALAEI ;BEATRICE MOTELLA ;ANDREW DEMPSTER

Abstract - In the Global Positioning System (GPS), Code Division Multiple Access (CDMA) signals are used. Because of the known spectral characteristics of the CDMA signal, Continuous Wave (CW) interference has a predictable effect on the different Pseudo Random Noise (PRN) spreading codes (unique to each satellite) depending on the Doppler frequency of the signal. The Doppler frequency for each signal is also predictable once the receiver position is known. As different satellite signals have different Doppler frequencies, the effect on the signal quality is also different. In this paper first the effect is studied analytically. The concept of an "exclusion zone" is defined and analyzed for each satellite. This exclusion zone, where that satellite should not be used due to interference degradation, is shown to be predictable for each satellite as a function of time. Using this prediction, the CW interference effect on the positioning quality of the receiver can be mitigated by ignoring the affected satellites within exclusion zones when performing position evaluation. The threshold beyond which a satellite should be excluded is then derived by studying the mutual effects of the geometry and the signal quality of that satellite on the positioning quality. Receiver Autonomous Integrity Monitoring (RAIM) uses redundancy in measurements to perform an internal consistency check to see if all of the measurements are satisfactory. In this paper this technique is also used to mitigate the effect of CW interference on the positioning accuracy. Finally it is shown that the prediction of the exclusion zone for each satellite outperforms the RAIM algorithm in mitigation the effect of the interference when 5 satellites are visible.

Keywords: GPS receiver; CW Interference; RAIM algorithm; carrier to noise ratio (C/No)

1. Introduction

Radio Frequency Interference (RFI) is amongst the most disruptive events in the operation of a GPS receiver. It affects the operation of the Automatic Gain Control (AGC) and Low Noise Amplifier (LNA) in the RF front-end (Kaplan

(1996) Bastide (2003)) and depending on how much of it passes through these primary modules, it can also affect the carrier and code tracking loops (Betz (2001) and Tabatabaei (2006a)) which results in deterioration of all the GPS observables or in complete loss of lock in severe cases. CW interference has been shown to have severe effects on the GPS C/A code signal (Spilker 1996). This is because the frequency spectrum of the C/A code signal has a series of vulnerable lines (Kaplan 1996). Interference can be detected in the receiver either before or after the correlation. Pre-correlation techniques use the antenna (Brown 1999), and Analogue to Digital Converter (ADC) (Amoroso 1983) to detect and characterize the RFI. In the post-correlation stage, the observables of the receiver that are affected by RFI have usually been used to detect and characterize the interference.

There are many different techniques for mitigation and suppression of interference. Antenna array processing, adaptive filtering (Abimoussa (2000)), time-frequency analysis and synthesis (Lijun (2005)) are among them. In Ndili (1998), interference is detected based on a combination of the following test statistics: correlator output power, variance of correlator output power, carrier phase vacillation, and AGC control loop gain.

Receiver Autonomous Integrity Monitoring (RAIM) is also considered as another mitigation approach (Dempster (2006)). Specifically for CW RFI, which can affect one satellite at a time, this technique proves to be effective. However, our ability to predict the impact of CW RFI on the signal quality of the GPS receiver can achieve better results than simply applying RAIM algorithms. Specifically in the static applications such as Continuously Operating Reference Stations (CORS) network base stations where the environmental characteristics such as multipath and interference models do not change, this proactive approach to monitoring the satellite signal quality and availability is shown to have advantages.

In section 2 the effect of CW on the carrier to noise ratio C/No is analytically studied and presented as a background to define the new concept of the satellite exclusion zone. In section 3, the elements of satellite positioning quality are studied to obtain an appropriate threshold to determine the exclusion zone. The proactive mitigation algorithm is also presented in this section. Section 4 is dedicated to the experiments to mitigate interference from real GPS signals

collected by a software GPS receiver using both a RAIM algorithm and the proposed preventative technique. Section 5 summarises the results.

2. The Effect of CW RFI on the GPS Signal Quality

In Tabatabaei (2006a), we derived an expression for the post-correlation carrier to noise density (C/No). Figure 1 shows a block diagram of the correlation process in the GPS receiver.

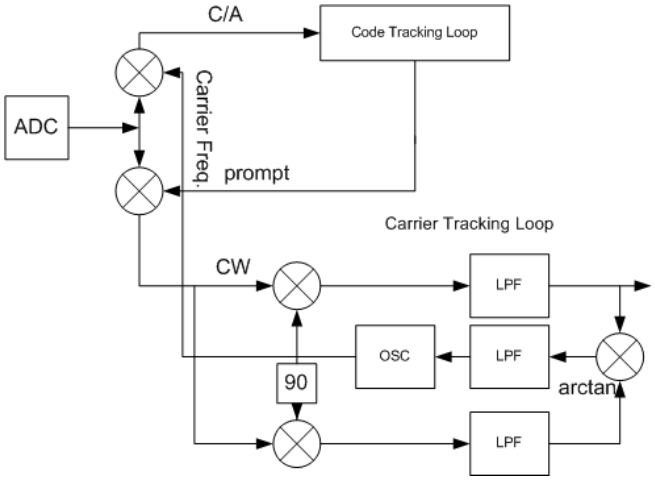

Figure 1 Correlator (Code and Carrier Tracking Loops)

Equation (1) shows the mathematical expression for the C/No at the output of the correlator (Tabatabaei (2006a)).

$$\mathrm{C/No} = \frac{(\sqrt{2P_s}T_d R_0(\tau).\mathrm{sinc}(\Delta f_c T_d))^2}{L_n N_0 + (J.T_d \mathrm{C}_\mathrm{n}^*.\mathrm{sinc}(\mathrm{T_d}.\Delta f_i))^2} \qquad (1)$$

where: P_s is the GPS signal power, $\mathrm{N_o}$ is the thermal noise power, J is the interference power, L_n is the processing gain applied to the noise, T_d is the integration duration time, $\hat{f}_c$ is the estimate of carrier frequency.

$\Delta f_c = f_c - \hat{f}_c$ and $\Delta f_i = f_i - f_c$ (f_i is the interference frequency), $\mathrm{C_n}$ is the $\mathrm{n^{th}}$ spectral line coefficient, $R_0(\tau)$ is the cross correlation of the received C/A code and the receiver estimate of the code and τ is the signal-reference code phase difference in code chips.

In Figure 2, as an example, using (1) and assuming a specific environmental noise power, the C/No is shown for satellite 1 with Doppler frequency changing from 0

kHz to 10 kHz and CW interference with a specific power at 14 kHz away from L1 frequency (i.e. at 1.575434 GHz).

The deep troughs in this graph correspond to the coincidence of CW RFI with the code spectral lines. It is clear that this happens at 1 kHz spacing in the Doppler frequency, as expected because the code repeats each 1ms. As expected from (1), there are different values for different lines. This difference comes from the difference between the coefficients of different lines in the code spectrum. This particular line spectrum would thus be different for different satellite codes. The other point which is noticeable in this figure is the inverted Sinc functions occurring around each trough. The width of each inverted Sinc function is related to the integration period, as can be seen in (1). The longer the integration period is the narrower will be the Sinc functions and the more immune the receiver will be to CW interference away from the code spectral lines (and the more vulnerable *at* the spectral lines).

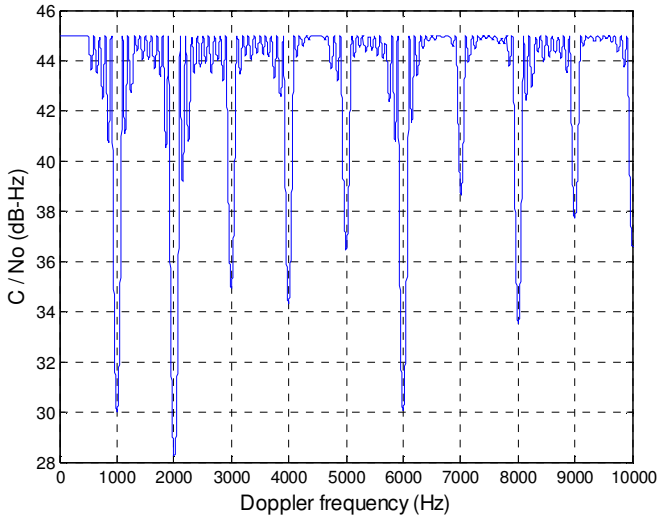

Figure 2 C/N0 calculated using the mathematical expression for satellite 1 with Doppler frequency changing from 0 kHz to 10 kHz and CW interference at 14 kHz away from L1 frequency

Figure 3 shows the variation of the Doppler frequency for different satellites for 24 hours for a specific almanac file in the presence of narrowband CW interference. Gaps in the plots indicate where an interferer in L1 frequency (or any integer multiply of 1 kHz away from that) may cause these signals to be "lost". Depending on satellite number, signal power, strength of the interference and the background noise power, the width of this gap changes. Instead of losing lock, we can set a threshold for the C/No which is a good indication of the signal quality.

For any value of C/No less than this threshold, that specific signal will be taken out of the operating channels. We call the zones that are achieved through this algorithm "exclusion zones". This is the frequency region in which the interference "knocks out" that satellite and the pseudorange for that satellite should be "excised" from the solution.

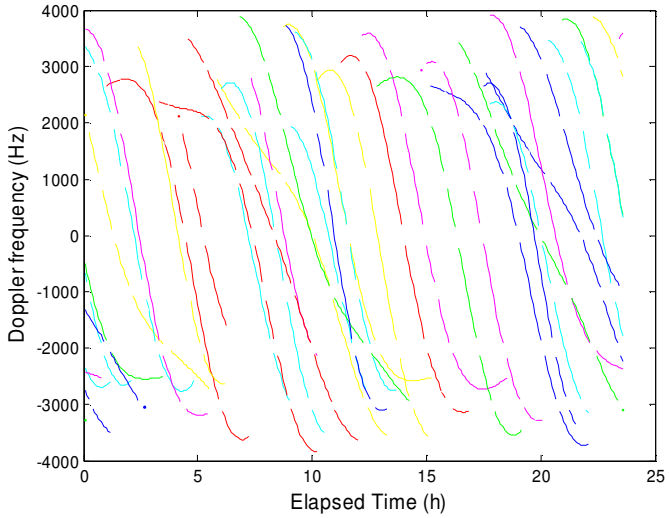

Figure 3 Variation of Doppler frequencies for the visible satellites over 24 hours. Exclusion zones are indicated at multiples of 1 kHz.

There are a number of different techniques for detecting the RFI and calculating its frequency and power. Statistical inference applied to the Fourier transform is a common technique which is used for this purpose in (Tabatabaei (2006b)). Once the exact frequency of the RFI is calculated, the second step is to find the exclusion zone for each of the lines. In Figure 4 this quantity is shown in terms of the corresponding trough depth in the C/No calculated theoretically (equation 1).
In this case, a conservative value of 40 dB-Hz is chosen for the C/No threshold. Obviously the more power in the spectral line, the greater the effect of the interference, and the deeper will be the trough in the C/No. The figure shows that the deeper the trough, the wider will be the exclusion zone for that satellite around that specific line. As an example, the first point in this graph shows 27.7 dB-Hz and 136 Hz. This means that if a trough with the depth of 27.7 dB-Hz is generated in the trend of C/No (like one of the troughs of Figure 2), then with the receiver threshold of 40 dB-Hz for C/No, the value of C/No is less than the threshold for 136 Hz of Doppler frequency change (note that the horizontal axis of figure 2 is Doppler frequency change of the satellite). So by using Figure 2 which provides

an idea of how to calculate the exclusion zone in terms of C/No and (1) with which we can calculate the C/No, the exclusion zone of any satellite signal at any Doppler frequency can be calculated.

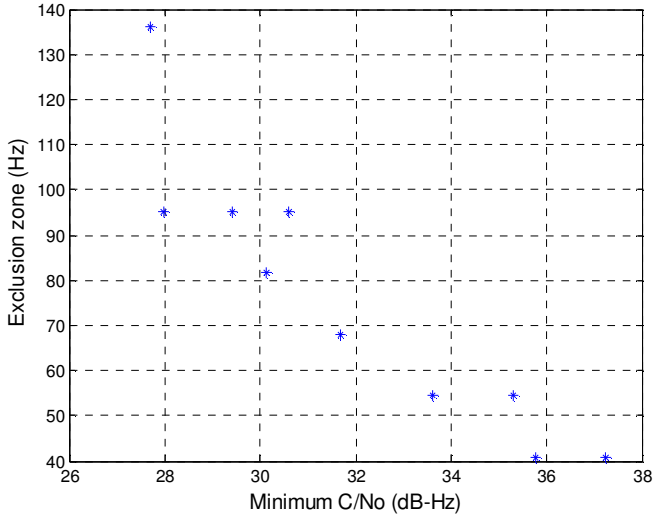

Figure 4 Relation between trough depths in C/No calculated theoretically and the corresponding satellite exclusion zone

In Figure 4, it can be seen that there is a relatively linear relationship between the exclusion zones of different C/A code spectral lines and the C/No trough depth which is calculated theoretically as the result of those lines. In the following experiment the NordNav software receiver is used to capture the IF data to be analyzed and post processed and a signal generator (HP8648B) is used to generate the CW interference which is combined with the GPS signal generated by a SPIRENT GSS6560. The aim of this experiment is to characterize the effect of interference power on the level of C/No (Tabatabaei (2006a)). The exclusion zone is characterized for just the two lines circled. Line one in Figure 5 corresponds to the 4^{th} spectral line of the code away from L1. So the 6^{th} and 7^{th} lines are at 9 and 10 kHz away from the band centre in this figure. Both the theoretical and the actual calculated C/No (using the I and Q samples from the NordNav software receiver) are shown to closely correspond to each other in this figure.

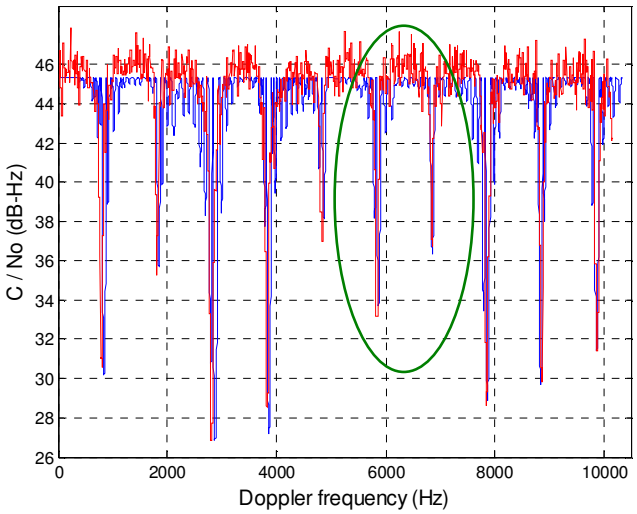

Figure 5 Actual C/No calculated using the I and Q samples (red) and Theoretical C/No calculated using 1 (blue) for PRN 1 and interference at 4 kHz away from L1

Instead of 10 kHz, the interference is moved only 2 kHz in 4 minutes (which guarantees crossing two 1 kHz lines separated by 2 minutes). In this experiment, the wideband noise power and the signal power are kept constant. The experiment is performed for four different RFI powers (Table 1).

RFI Power/ exclusion zone	- 82dBm	- 85dBm	- 88dBm	- 91dBm
Line 1	94 Hz	87 Hz	22 Hz	0 Hz
Line 2	101 Hz	95 Hz	14 Hz	7 Hz

Table 1 Exclusion zones for four different RFI powers for two consecutive C/A code spectral lines

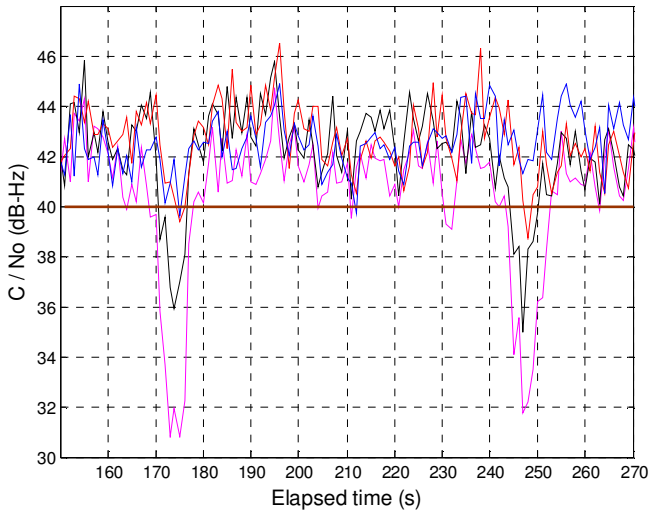

Figure 6 C/No for four different values of RFI power (magenta, black, blue and red for -82, -85, -88, -91 dBm respectively)

In **Error! Reference source not found.**, the effect of these four power levels of RFI is shown on the C/No. It is obvious that where the RFI lines up with the C/A code spectral line, the higher power has the more serious effect. The other thing that can be seen from **Error! Reference source not found.** is that where the RFI does not line up with the C/A code line, the power of RFI does not have a significant effect on the C/No. In other words CW RFI affects C/No only when it lines up with the C/A code line. In Table 1, it can be seen that the exclusion zone for the two lines increases with increasing power of RFI. This is expected, as the depth of the trough is greater for greater RFI power, and the width is also greater.

3. Positioning Quality Elements

Satellite geometry and satellite signal quality, mathematical approach

The accuracy of positioning, using the measured pseudoranges from the receiver to each of the satellites, depends on several different factors. The position evaluation in the GPS receiver estimates four quantities (x, y, z and time) using four or more pseudoranges. Briefly there is the following relationship between the pseudorange error ($\Delta\rho$), position error (Δx) and the geometry matrix (G) (Parkinson (1996a)).

$$\Delta x = (G^T G)^{-1} G^T \Delta\rho \qquad (2)$$

It is easy to see in this equation that the position accuracy is decided by two factors, the measurement quality and the user-to-satellite geometry. These factors separately are extensively discussed in (Parkinson (1996a)). In this section we will make a quantitative comparison of the effect of each one of these two factors on the positioning accuracy. The aim is to establish if pseudorange error is large because of the poor signal quality (low C/No), under which circumstances we can achieve better position accuracy by eliminating that satellite, noting the fact that eliminating the satellite will affect the geometry.

To achieve this goal, we simplify the scenario. The assumption is that there are 5 satellites available to the receiver and of these only one has affected signal quality. This means that only this satellite is affected by interference. This situation is likely to occur when there is moderate blockage of sky and a single CW interferer is present. The position error covariance is studied in this investigation: $\mathrm{cov}(\Delta x) = E(\Delta x \Delta x^T)$ where *E(.)* operates as an expected value operator. From (2) we have:

$$\mathrm{cov}(\Delta x) = E((G^T G)^{-1} G^T \Delta\rho \Delta\rho^T G (G^T G)^{-1}) \qquad (3)$$

At this stage two different cases are considered: 4 satellites all having the same pseudorange error (ε) and 5 satellites one of which has a degraded signal with larger pseudorange error (η). Without loss of generality we can assume here that the pseudorange error in the first case for each satellite is $\varepsilon = 1$ m and that of the second case to be $\xi = \eta / \varepsilon = \eta$. Then for the two cases we will have:

$$\mathrm{cov}_4(\Delta x) = (G_4^T G_4)^{-1} (G_4^T W_4(\xi) G_4)(G_4^T G_4) \qquad (4)$$

where $W_4(\xi) = I_4$

and

$$\mathrm{cov}_5(\Delta x) = (G_5^T G_5)^{-1} (G_5^T W_5(\xi) G_5)(G_5^T G_5) \qquad (5)$$

where $W_5(\xi) = \begin{bmatrix} I_4 & 0 \\ 0 & \xi^2 \end{bmatrix}$.

G_4 and G_5 represent the G matrix respectively for the cases of 4 and 5 satellites.

The difference between the above two quantities comes from the difference between G_4 and G_5 on the one hand and W_4 and W_5 on the other. In the scenario explained in the following section, the effects on the position error covariance of W and G are studied.

The data used for this scenario are a set of real data collected with a GPS software receiver NordNav-R30 at the University of the New South Wales on the 6th November 2006. Six satellites (1, 11, 20, 23, 25 and 31) are acquired by the receiver.

To compare the covariance matrices (4-5), one way is to compare their determinants. Two satellite sets of (1, 23, 25, 31) and (1, 11, 23, 25, 31) are chosen. These two sets are chosen because during the initial epochs of the data, satellite 11 plays a fundamental role in delivering good geometry of the constellation. In this experiment, as explained earlier, only the pseudorange error of the satellite 11 is changed. By using (4) and (5), the amount of pseudorange error of satellite 11, which makes the position error for the two configurations equal, is found to be $\xi_0 = 22\,m$. Figure 7 shows the position error for the two cases with respect to the pseudorange error of satellite 11 with (blue) and without (red) the use of this satellite in the positioning calculations. It is obvious that the position error should not change by changing the pseudorange error of satellite 11 (red) whereas it should change in the case where satellite 11 is considered in the positioning calculations (blue). It is clearly seen that the position error for the two configurations (4 satellites and 5 satellites) become equal to each other at $\xi_0 = 23.1\,m$ which is very close to what is predicted theoretically.

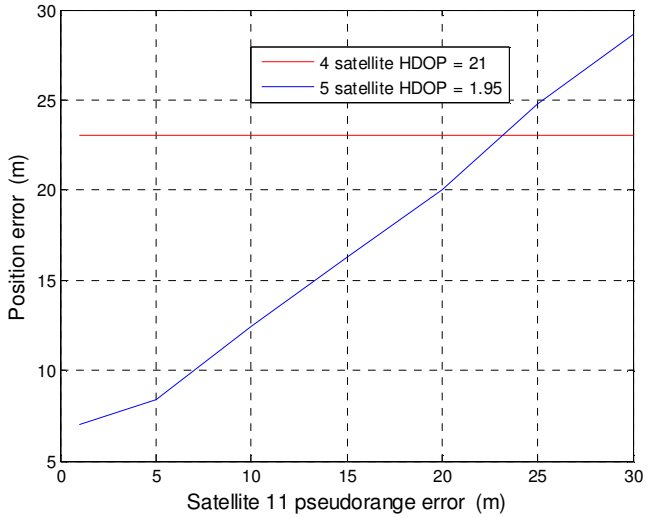

Figure 7 Position error vs. pseudorange error for the 4 and 5 satellite configuration at a particular time

In another scenario, another two satellite sets are chosen which have very similar and good geometries. These two sets are (1, 11, 20 and 23) and (1, 11, 20, 23 and 25). The satellite of which the pseudorange error has been increased is satellite 25. Again using (4) and (5), the pseudorange error at which the two position errors become equal is calculated. This error is found to be $\xi_0 = 1.45\,m$. Figure 8 shows that this value in the experiment was found to be 1.65 *m.* This means that there will be times when eliminating the satellite because of its poor CNo will have advantages and others when the degradation has to be significant before elimination helps.

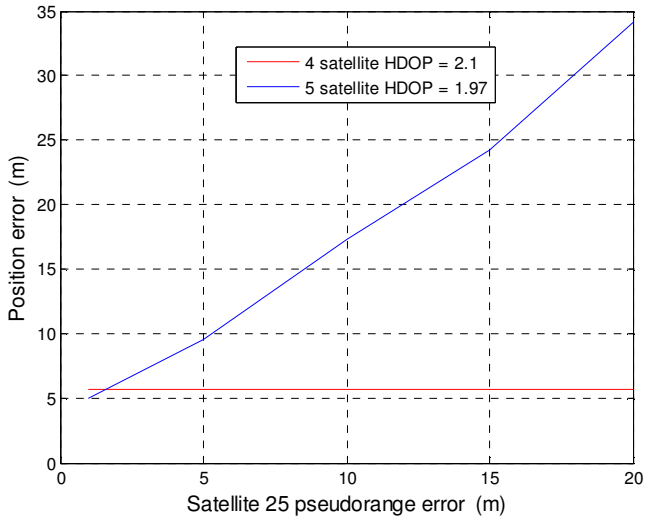

Figure 8 Position error vs pseudorange error for the 4 and 5 satellite configuration

Mitigation algorithm description

Here the algorithm for the proposed technique to mitigate the effects of CW interference is described.

1) As was explained in section 2, using the information regarding the frequency and power of the interference and the constellation information, the carrier to noise ratio of each channel is predicted using (1).
2) Using (4) and (5), for each of the satellites in view, the minimum pseudorange error at which the positioning error becomes higher when including that particular satellite is found. This value is called ξ_0. Here it is assumed that the relationship between the pseudorange error and the carrier to noise ratio for the GPS receiver in which this algorithm is used, is known (Ndili (1998)). Usually the pseudorange is calculated using the code phase so what is really important is to see the effect of the interference on the code tracking error. This has been done in Betz (2000). Different techniques are discussed in that paper regarding the code phase error among which is the effect of C/No on this parameter. Also in Kaplan (2006), a lower bound is given for code tracking error in terms of C/No which is even independent of code tracking system design.
3) If the predicted carrier to noise ratio of a satellite is less than the value which corresponds to ξ_0 m pseudorange error, then that satellite will be excluded from the positioning evaluation.

This process is schematically shown in Figure 9.

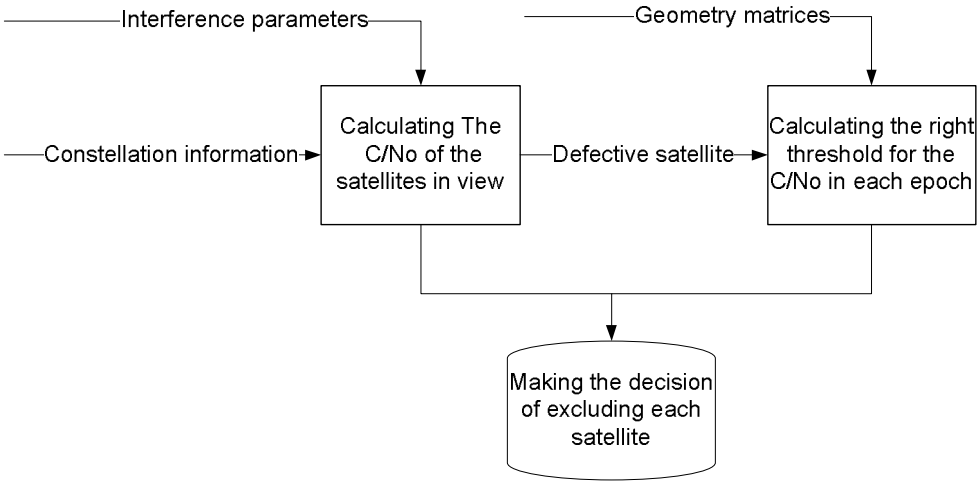

Figure 9 Algorithm description flow chart

It was shown in section 2 that degradation in satellite signal quality (C/No) due to interference can prevent one or more satellites being available. In Fante (2000) the probability of availability of N satellites in the presence of interference in terms of C/No was investigated. Due to the nature of this impact of CW RFI on the GPS satellite signals, one can reasonably think of using a RAIM algorithm to mitigate this effect. In Kim (2006) the position domain errors are assessed with the use of traditional least-squares estimation in the presence of interference, mitigated by a RAIM scheme. Also in Yun (2006), an RFI mitigation technique is introduced based on integrity monitoring for a Differential GPS (DGPS) system.

In this section the dependency of our proposed mitigation algorithm on the satellite geometry was studied. Also in Brown (1990) the dependency of RAIM on geometry is discussed. So in the fact that the two algorithms are dependent on the geometry they are similar but there are differences between the two mitigation techniques which in the next section using some experiments are analyzed and discussed.

4. Experiment Discussion and Results

The impact of the HDOP

The goal of this section is to demonstrate the theoretical analysis discussed in sections 2 and 3 with some experiments. The data used for this purpose are the same of those have been used for the simulation results. The question to be

addressed is in which cases the 'exclusion zones' algorithm can be applied. In other words: what is the trade-off between the loss of positioning accuracy due to degraded geometry and a loss of position accuracy due to the use of the satellite affected by CW interference? This is then used to decide if the affected satellite should be eliminated from position estimation. By analyzing the following two examples this question is approached.

In the first example we analyze the possibility of applying the 'exclusion zone' algorithm in the case where the HDOP is comparable before and after excluding one satellite. The constellation considered is composed of satellites 1, 11, 20, 23 and 25. The CW interference affects the signal of satellite 1. It can be seen from Table 2 that the value of the HDOP does not change significantly when satellite 1 is removed. In fact the HDOP for both cases stays almost constant for the 38 minutes of data.

HDOP - 5 sat	HDOP - 4 sat
1.97	2.07

Table 2 HDOP for the 5 and 4 satellite configuration

The position error is described versus time (Figure 10 a) on the scatter diagram (Figure 10 b). Blue lines refer to the 5 satellite configuration, while red lines refer to the position error evaluated omitting satellite 1.

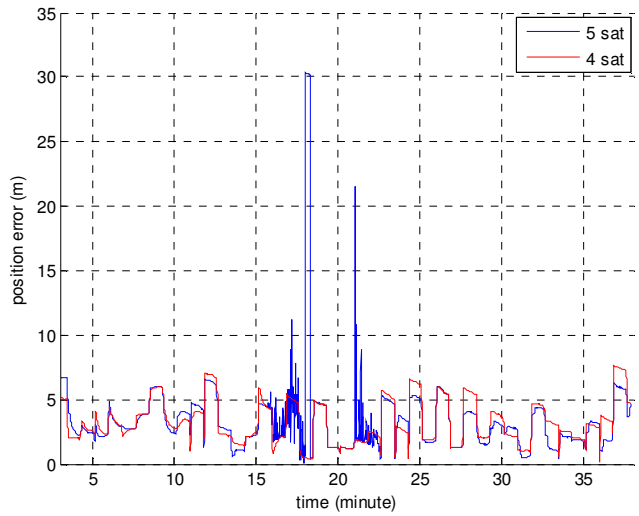

(a)

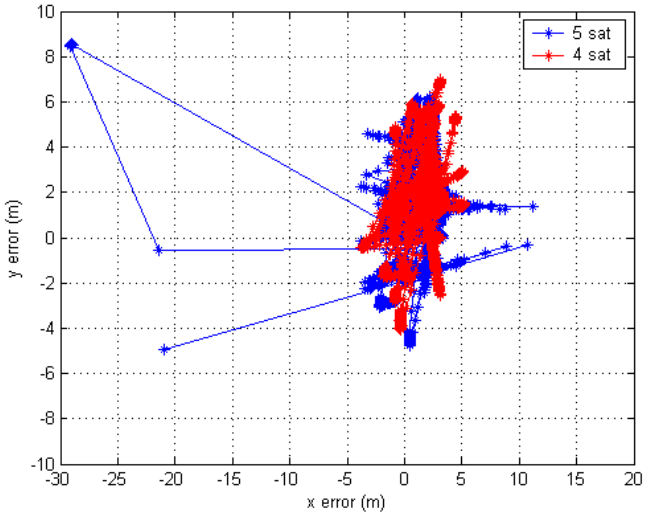

(b)

Figure 10 Position error vs. time (a) and scatter diagram (b). The comparison is between the 5 satellites configuration (blue line) and the 4 satellite one (red line) when the interference affects the satellite 1 (kept out in the 4 sat configuration)

It is observed that the performance of the 4 satellite configuration is comparable with the 5 satellite ones, except where the interference matches one of the lines of the PRN 1 code (between min 16 and min 22).

On the contrary, the second example analyses the case where the HDOP varies significantly after removing one satellite. The constellation is composed of satellites 1, 11, 20, 25 and 31. The CW interference affects the C/No of satellite 11 (Figure 11 (a)). Moreover in the 4 satellite configuration the value of the HDOP varies from 22.5 to 4 during the 38 minutes (Figure 11 (b)).

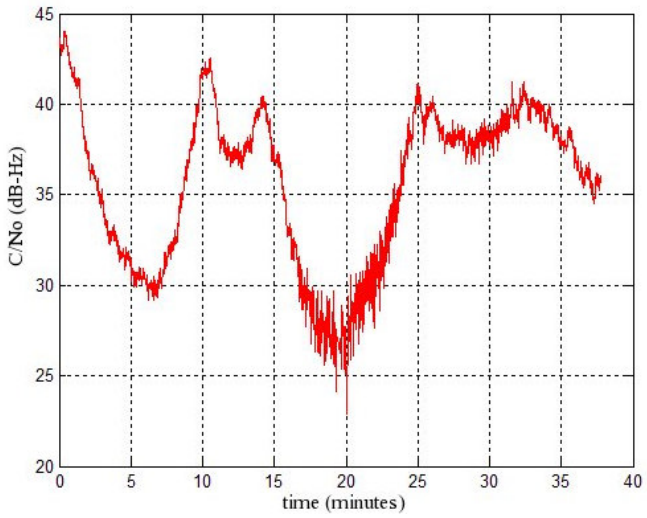

(a)

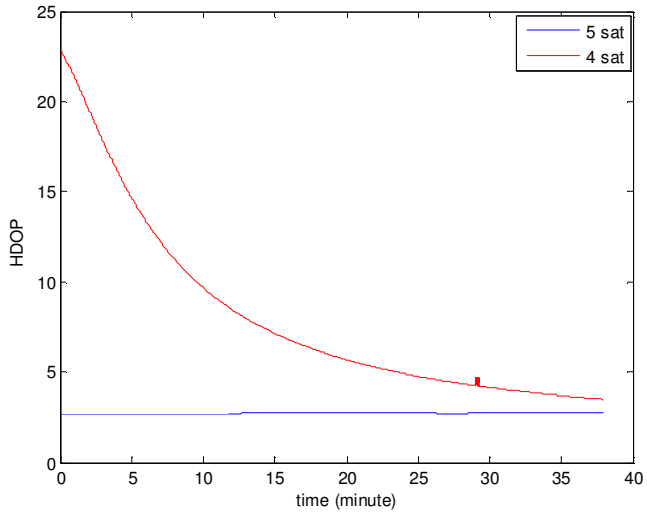

(b)

Figure 11 C/No for the PRN 11 (a) HDOP for the 5 and 4 satellites configuration (b)

During the first 18 minutes the difference between the HDOP of the two constellations is very high. This means that the HDOP of the 4 satellite configuration is extremely high and this is reflected in a very high position error (see Figure 12). The maximum error in this case is 35 m and it exceeds 15 m several times. With this level of position accuracy there is no reason to apply the exclusion zone algorithm, because the HDOP does not allow acceptable position estimation.

On the contrary, when the difference in HDOPs is not significant (less than 7 after min 18), it is easy to observe that the performance of the 4 satellite configuration, after the application of the exclusion zone algorithm, is much better than the 5 satellite configuration when the interference matches one of the lines of the PRN

11 code (Figure 12 (a)). Note that the interference is present throughout the experiment. In order to see how much the interference can affect the position accuracy Figure 12 (b) represents the difference with and without interference.

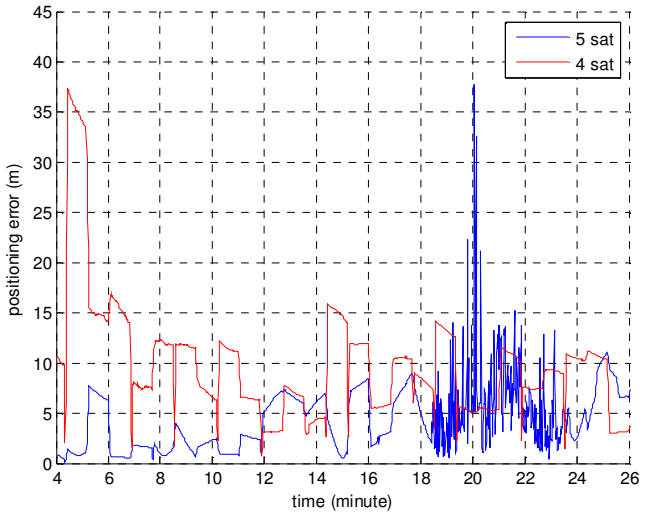

(a)

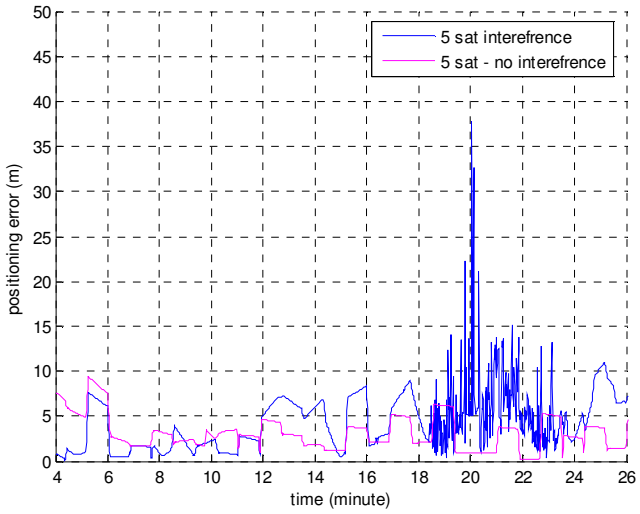

(b)

Figure 12 Comparison between the positioning error using 5 and 4 satellites in presence of interference (a) Comparison between the positioning error using the 5 satellites constellation with and without interference (b)

Exclusion Zone – RAIM Comparison

In order to show the advantages of the 'exclusion zone' algorithm in comparison to a RAIM technique, an example is shown. The maximum solution separation RAIM method (Parkinson (1996b)) has been chosen for the comparison.

To apply the exclusion zone algorithm, we consider the example in the previous subsection, (Figure 10). In Figure 13 (b), which is the trend of the C/No of satellite 1, it is observed that the decision to exclude the satellite cannot be based only on measuring the actual C/No level. This level is in fact always quite high (> 34 dB-Hz) even when the position quality is severely affected by the interference. This is explained in Tabatabaei (2006a) where the behavior of C/No in the presence of CW interference is characterized. It is shown that this type of interference has an "improved" effect on the C/No, when its frequency is very close to the frequency of one of the lines of the C/A code. The reason is that the carrier tracking loop tracks the interference and the stronger the interference, the higher will be the C/No. On this basis, the C/No by itself can be a misleading indicator in this specific situation.

Instead of monitoring the C/No, by predicting the C/No this problem is resolved. In this experiment the frequency of the CW RFI is chosen so that the signal of GPS satellite 1 is affected significantly during the course of the 38 minutes. The Doppler frequency of this satellite is shown in Figure 13 (a). The interference is chosen to be at frequency 12.1 kHz away from L1. As the Doppler frequency of this signal is 2 kHz, so the RFI will coincide with the 10^{th} spectral line of this code in the middle of the experiment. The RFI power is chosen to be -82 dBm because this guarantees C/No degradation – see Table 1.

In section 3, we proposed a method to calculate, at any given time, the C/No threshold ξ_0 at which a satellite should be excluded. Following that analysis, ξ_0 for this specific case is 2.1 m. In the next step the carrier to noise ratio, corresponding to this level of pseudorange error should be found. In (Ndili (1998)) the relationship between pseudorange error and the correlator output power or the C/No is characterized. This relationship varies based on the receiver.

The fact that ξ_0 is very close to 1 m means that satellite 1 does not have a significant effect on the geometry and therefore should be excluded from the positioning calculation as soon as the positioning error is affected by the poor signal quality. For this specific PRN code line and RFI power level and the threshold, the exclusion zone from (1) is found to be 101 Hz (Figure 13). Again the RFI is present throughout the experiment. However its detrimental effect is worst only during the exclusion zone. As it is clear from Figure 10, the position

error has been improved significantly after applying this technique. In Table 3, this improvement is quantified.

Table 3 Maximum position error before and after applying the mitigation technique

Maximum position error before applying the preventative RFI mitigation	Maximum position error after applying the preventative RFI mitigation
30.5 meter	7 meter

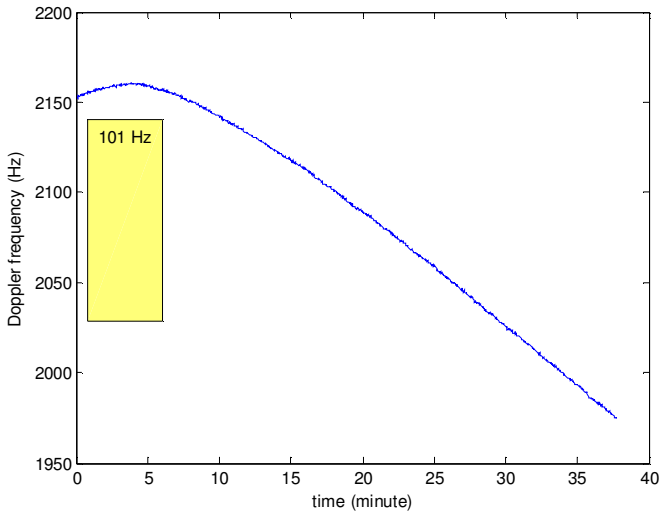

(a)

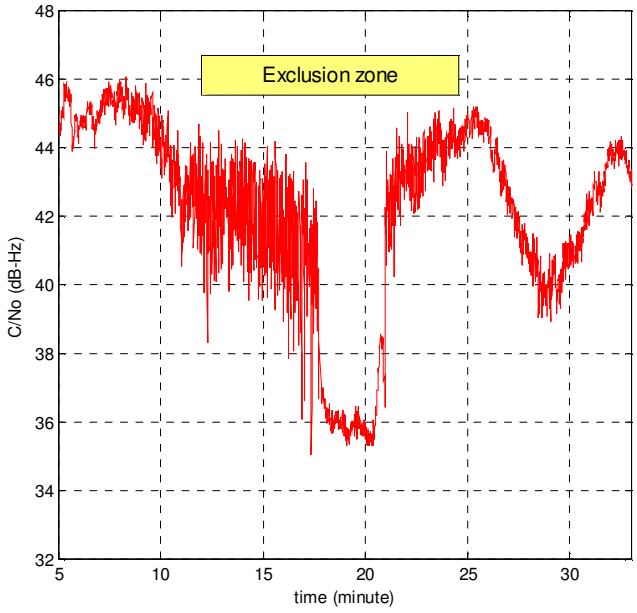

(b)

Figure 13 (a) Doppler frequency for PRN 1 (b) Exclusion zone for PRN 1

The advantages of this algorithm are most appreciable when we have only 5 satellites in view. This is because in this situation the RFI affected satellite can have a stronger effect on the positioning quality whereas for higher numbers of satellites, it is possible that even though the affected satellite does not have significant effect on the geometry, elimination of that satellite does not improve the positioning quality either. This is shown schematically in another scenario from the same data. We have 6 satellites in view, (PRN 1, 11, 20, 23, 25 and 31). Using the exclusion zone algorithm, we know that the signal from satellite 1 can be seriously damaged by the presence of the interference at a particular time – we also know the other satellites are not affected in this way.

Figure 14 (a) and (b) show the position error before and after the exclusion zones in the scatter plot and versus time respectively.

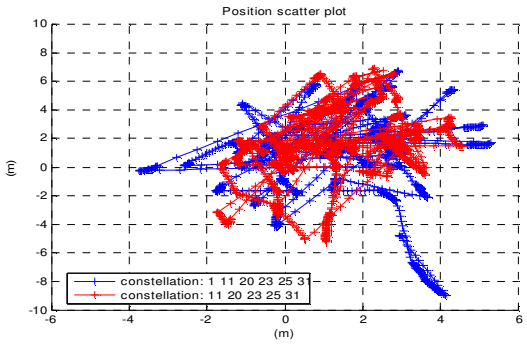

(a)

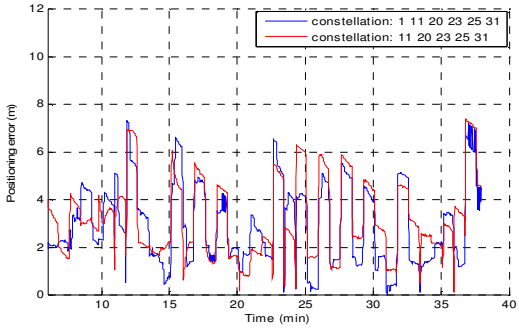

(b)

Figure 14 Position error for 6 satellites, one of which is affected by interference – scatter plot (a) Positioning error before and after the exclusion zone (b)

The advantage of removing satellite 1 from the position estimation does not bring big advantages in terms of position accuracy.

As we saw in the first example, the advantages of the algorithm became more appreciable when we have only 5 satellites in view.

The RAIM algorithm needs at least 5 satellites to detect the presence of an error in one of the pseudorange and 6 satellites to identify which is deficient.

In order to compare the exclusion zones algorithm with RAIM, the situation with 5 satellites in view is analyzed. Figure 15 shows the maximum distance between the five position solutions evaluated removing one satellite at a time (constellation: PRN 1, 11, 23, 25, 31).

In this case it is difficult to detect the presence of the error using the maximum distance of solutions algorithm. The different positions are evaluated using only 4 satellites. This means that the HDOP can significantly affect the accuracy in the positioning evaluation. In other words, the effect of poor HDOP is more than the effect of the existing interference and between minute 16 and minute 22, the maximum separation distance is not higher than the other time where RFI has no effect. Therefore in this experiment, even though 5 satellites are available, because of poor geometry, the presence of error caused by interference can not be detected.

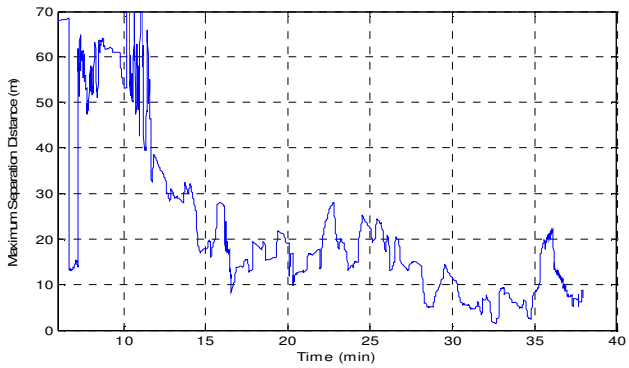

Figure 15 Maximum distance between positioning from different satellite configuration for the 5 satellite set, one affected by interference

Here of course the investigation is carried out on a particular real data example. In this example it was shown how the “exclusion zone” algorithm results in significant improvement of the positioning quality for low numbers of satellites. RAIM algorithms are not competitive in those situations because of lower redundancy which is essential to RAIM algorithms.

5. Summary

In this paper a new technique to mitigate the effects of CW interference on GPS C/A code signal quality is introduced. No analogue or digital filter is used in this

algorithm and this helps keep the GPS signal phase and amplitude from being distorted. Unlike other mitigation techniques which are responsive, this technique works preventatively but it does require knowledge of the interference frequency and power, which may be estimated by known techniques plus the relationship between the C/No and the pseudorange error for the receiver. This means that it predicts and prevents the error before it happens. The specific signal structure in GPS allows us to predict the effect of CW interference on each of the satellites' signal (C/No) at any given time. It usually affects one signal at a time and in the technique proposed in this paper that affected satellite is removed from the positioning calculations provided that its C/No is less than a threshold. This threshold depends on the effect of that satellite on the user-to-satellite geometry.

Receiver autonomous integrity monitoring techniques work on a similar basis. The difference is that in the RAIM approach the affected signal is detected after the error appears in the positioning calculations. The other difference between the RAIM technique and the proposed preventative algorithm is that RAIM needs a higher number of received satellites whereas the preventative approach is effective in the presence of few satellites. It is shown in a case study that in the five satellite case, the positioning error was improved from 30 m to 7 m. For that example the maximum solution separation RAIM algorithm could not identify the error caused by the interference.

Reference

Abimoussa R, Landry RJ (2000) Anti-jamming solution to narrowband CDMA interference problem Canadian Conference on Electrical and Computer Engineering. Vol.2 Halifax, NS, Canada March 2000, pp 1057-1062

Amoroso F (1993) Adaptive A/D converter i o suppress co-channel constant envelope interference in a mobile digital link, Telecommunication Systems-Modeling, Analysis, Design and Management, vol. 2, no. 1, pp 109-19, 1993.

Bastide F, Akos D, Macabiau C, and Roturier B (2003) Automatic Gain Control (AGC) as an Interference Assessment Tool, Proceedings of ION GPS 2003, Portland, OR, September 9-12, pp 2042-2053.

Betz JW (2001) Effect of Partial-Band Interference on Receiver Estimation of C/N0: Theory in Proc. ION 2001, Institute of Navigation, Long Beach, CA, January 22-24. 2001, pp. 16-27.

Betz JW (2000) Effect of narrowband interference on GPS code tracking accuracy," in Proc. of ION National Technical Meeting, Anaheim, CA, Jan. 2000, pp. 16 – 27.

Brown A, Reynolds D, Roberts D, Serie S (1999) Jammer and Interference Location System - Design and Initial Test Results, Air Force Space Battlelab, Proceedings of the ION GPS Nashville, Tennessee. pp. 137-142

Brown A, Sturza M (1990) The effect of geometry on integrity monitoring performance Institute of Navigation (ION) Annual Meeting; Atlantic City, New Jersey pp. 121-129

Dempster A (2006) How Vulnerable is GPS? Position, no 20, Dec 2005/Jan 2006, pp64-67

Fante RL, Vaccaro JJ (2000) Ensuring GPS availability in an interference environment. Position Location and Navigation Symposium IEEE San Diego, CA, USA pp. 37-40

Kaplan E (1996) Understanding GPS: Principles and Applications. Artech House.

Kaplan E, Hegarty C (2006) Understanding GPS: Principles and Applications, Artech House

Kim N (2006) Interference Effects on GPS Receivers in Weak Signal Environments. University of Calgary, Department of Geomatics Engineering Masters Thesis.

Lijun W, Huichang Z, Gang X, Shuning Z (2005) AM-FM interference suppression for GPS receivers based on time-frequency analysis and synthesis IEEE International Symposium on Microwave Antenna, Propagation and EMC Technologies for Wireless Communication, MAPE 2005. Volume 2, pp. 1378 - 1381

Ndili A, Enge P (1998) GPS receiver autonomous interference detection. Position Location and Navigation Symposium, IEEE Palm Springs CA, 20-23 April 1998 pp123 - 130.

Parkinson BW, Spilker JJ Jr (1996a) Global positioning system: Theory and Applications Volume I, American Institute of Aeronautics and Astronautics, Inc.

Parkinson BW, Axelrad P, Enge P (1996b) Global positioning system: Theory and Applications. Volume II

Spilker J, Natali F (1996) Global Positioning System: Theory and Applications. AIAA

Tabatabaei Balaei A, Barnes J, Dempster A G (2006a) A Novel Approach in the Detection and Characterization of CW Interference on the GPS Signal Using the Receiver CN0 Estimation. Proceeding of IEEE/ION PLANS, San Diego pp. 1120 - 1126

Tabatabaei Balaei A, Dempster A G (2006b) A Statistical Inference Technique for GPS Interference Detection Submitted to the IEEE Transaction on Aerospace and Electronic systems. November 2006

Yun Y, Kee C, Rife J, Luo M, Pullen S and Enge Per (2006) Detecting RFI Through Integrity Monitoring at a DGPS Reference Station The Journal Of Navigation, 59, pp. 403–422.